International Journal of Fatigue 21 (1999) S233–S246

International Journal of Fatigue

www.elsevier.com/locate/ijfatigue

Analysis of overload effects and related phenomena

K. Sadananda [a,*], A.K. Vasudevan [b], R.L. Holtz [a], E.U. Lee [c]

[a] *Code 6323, Materials Science and Technology Division, Naval Research Laboratory, Washington, DC 20375, USA*
[b] *Office of Naval Research, 800 N. Quincy Street, Arlington, VA 22217, USA*
[c] *Naval Air Warfare Center Aircraft Division, Code 4342, Unit 5, Patuxent River, MD 20670, USA*

Abstract

Overloads and underloads perturb steady state fatigue crack growth conditions and affect the growth rates by retarding or accelerating the growth. Clear understanding of these transient effects is important for the reliable life prediction of a component subjected to random loads. The overload effects have predominately been attributed to either plasticity induced crack closure behind the crack tip, residual stresses ahead of the crack tip, or a combination of both. These effects are critically examined in the context of the Unified Approach proposed by the authors. Recent experimental and analytical evaluation of crack closure has confirmed its negligible contribution to crack growth and has demonstrated that changes in the stresses ahead of the crack tip are more important than closure behind the crack tip. It is shown that the overload effects and other transient effects arise due to perturbation of the stresses ahead of the crack tip, and these can be accounted for by the two parametric approach emphasized in the unified theory. It is shown that related phenomena including the role of K_{max}, the existence of propagation threshold K_{pr}, and effects of overloads on K_{pr} and K_{max} etc, are all accounted for by the Unified Approach.

Keywords: Fatigue; Threshold; K_{max}; Overload; Crack closure; Residual stress

1. Introduction and background

Load bearing components in service rarely experience load amplitudes that remain constant during the length of the service. Since fatigue crack growth is driven predominantly by crack tip plasticity, and plastic strains are inherently irreversible, changes in the load patterns invariably result in transient effects which affect fatigue crack growth rates and hence the fatigue life. Quantification of these transient effects has been the subject of intensive study for more than three decades. Continued lack of reliable methodology to predict these transient effects exemplifies the complexity of the problem. Crack growth rates are known to be affected by superimposed overloads, underloads, variable amplitudes and block loads. The success of the fracture mechanics approach, both as a design tool and as a tool for prognostics, rests squarely on success of the analytical approaches to quantify these transient effects. In this paper, we use the term 'the overload effect' in a generic sense to denote not only the effects under spike overloads but also the effects during all transient conditions.

A superimposed single overload or spike load during constant load amplitude (or constant ΔK) fatigue is the simplest case of superimposed transient effect. Overloads are known to retard crack growth. The retardation effect depends on several factors, including the material flow properties, slip planarity and microstructure. Extensive work has been done in evaluating the effect of a single overload in terms of the number of delayed cycles required to revert to the background steady state crack growth rates. Some general observations can be made and these are summarized below as well as schematically in Fig. 1.

1. Overloads produce retardation while underloads produce acceleration relative to the background growth rates. Combined overload–underloads have mixed effects, depending on the sequence. These load–load interactions are complex and require careful experimentation and interpretation before quantitative predictions can be made.
2. The retardation generally is measured in terms of delay cycles, N_d, before the original steady state conditions are reestablished, see Fig. 1(b).

* Corresponding author. Tel.: +1-202-767-2117; fax: +1-202-767-2623.
E-mail address: sadananda@anvil.nrl.navy.mil (K. Sadananda)

0142-1123/99/$ - see front matter
PII: S0142-1123(99)00094-8

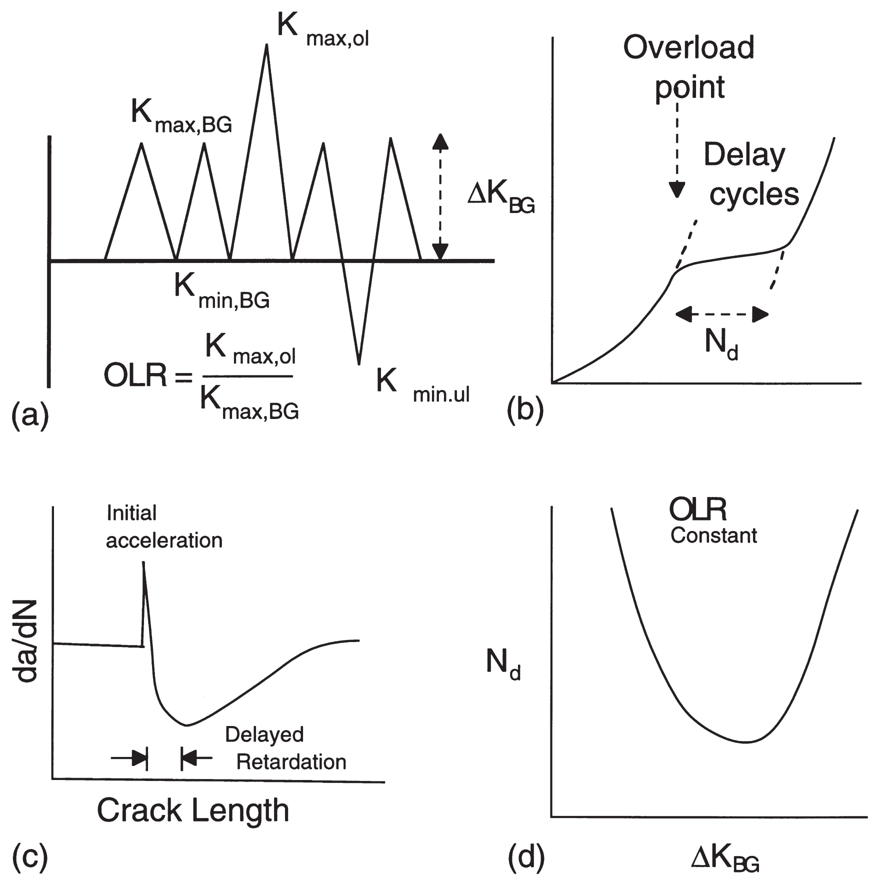

Fig. 1. Schematic illustration of the overload effects on fatigue crack growth.

3. The retardation effect depends on the overload ratio (OLR), K_{max} (OL)/K_{max} (BG), the background ΔK value at which the spike load is applied, and the background R-ratio.
4. While the transient effects always should, in principle, exist for any overload, measurable effects are observed only if the OLR exceeds some minimum value, typically at least 50%.
5. Overloads can produce a very short initial acceleration before significant deceleration occurs, Fig. 1(c). This initial acceleration is observable only at high OLR and depends on the material flow behavior. This can be seen clearly in a constant ΔK test, Fig. 1(c).
6. Maximum deceleration of growth rates occurs a short distance away from the point of overload, and this effect is termed as delayed retardation, Fig. 1(c). This delayed retardation depends again on the OLR and the background ΔK and R.
7. For the same OLR, N_d reaches a minimum as a function of the background ΔK, Fig. 1(d).
8. Retardation persists until the crack has propagated out of the perturbed plastic zone, a distance related to both the background plastic zone and the spectrum of the overload. Therefore, N_d depends on both the background plastic zone and the overload plastic zone sizes. Predictive models take advantage of these relationships.
9. Retardation effect depends on the specimen thickness since plastic zone size, PZS, under plane stress and plane strain differ. Retardation effects generally are larger under plane stress conditions.
10. All factors that influence the plasticity at the crack tip will have direct or indirect effect on overload effects. These include specimen geometry, temperature, environment and material properties. The extent of systematic work in this area is limited.
11. Since interactions between plastic zones are non-linear, sequential effects of overloads, under loads, block loads, periodic over and under loads are not easily amenable to quantification. However, for engineering approximations, one can arrive at some general rules that help in the quantification of the transient effects and hence in life prediction. Work in this area is somewhat sketchy, requiring a systematic effort for sorting and for improving the reliability of life prediction methods. The analysis is further complicated by the lack of consensus in the fatigue community in terms of the dominant mechanisms involved.
12. Various degrees of curve fitting approaches have been used in the literature to quantify the overload

effects and hence are predominately empirical in nature. Basic understanding of the problem is therefore essential before further progress can be made.

2. Mechanisms of overload retardation

With this background, it will be useful to examine the current explanations of the overload effects, since these manifest in life prediction models that are being proposed or developed. The central issue is the change in the crack tip driving force by the alteration of the steady state conditions at the crack tip by overloads. These have been reviewed extensively [1] but summarized here for clarity. The suggested mechanisms are based on experimentally observed materials behavior. These are listed below:

1. Crack tip blunting
2. Crack deflection, branching, and secondary cracking
3. Crack tip strain hardening or residual stresses ahead of the crack tip
4. Plasticity-induced closure
5. Roughness-induced closure

Mechanism (1) pertains to the changes in the geometry of the crack tip while (2) pertains to changes in the crack plane. Mechanism (3) is relatable to the alteration of the stresses ahead of the crack tip that affect either slip that is required for subsequent fatigue crack growth, or directly crack growth itself. Thus mechanisms (1) to (3) involve mainly transient conditions at or ahead of the crack tip. Mechanisms (4) and (5) operate behind the crack tip indirectly affecting the crack tip driving force. Some or all of these mechanisms may be acting simultaneously in any particular instance, but for the consideration of life prediction models under service loads it is most worthwhile to identify and consider the most dominant mechanism.

Overloads cause crack tip blunting affecting (a) crack growth that requires re-sharpening of the crack tip and (b) the stresses in the immediate vicinity of the crack tip. Blunting will have effects until the crack growth increment exceeds the crack tip radius during blunting. Indications [2–4] are that these effects may be important to some extent at high overloads in ductile materials. This mechanism does not predict (a) immediate acceleration after overload observed in some cases and (b) effects beyond the length scales of the crack tip curvature.

Crack tip branching, deflection and secondary cracking affect crack tip driving force [3,5] because Mode II and Mode III components are superimposed on Mode I. The mechanisms [6] are important for materials with significant planarity of slip and these mechanisms can be accentuated by certain environment or microstructures. However, these mechanisms are not sufficiently general and cannot account for the generic behavior observed under overloads. The tortuous crack path due to crack meandering can lead to roughness induced crack closure (mechanism (5) above). In addition, the decreased driving force after overload can activate the near-threshold mechanisms [7] involving faceted modes of crack growth in some planar slip materials, thus retarding the growth further by crack tip tortuosity and roughness induced closure. However, these effects a result of the decrease in driving force produced by overloads rather than the cause, which is the point of discussion here.

Crack tip strain hardening affects the initiation of further slip by the increase of flow stress [8]. This retards crack growth if the growth is activated by slip. On the other hand, if the crack grows by brittle types of mechanisms (for example, environmental effects), work hardening can have an opposite effect. In reality, the effects of strain hardening are not different from the compressive residual stress effects, since both are the same manifestations, but expressed slightly differently. The extended plastic zone formed during overload induces backward force at the crack tip (crack tip shielding) and hence future slip from the crack (dislocation nucleation and movement) has to overcome this backward force induced by the plasticity ahead. This is expressed as strain hardening mechanism resulting in increased flow stress. The same backward force, at the crack tip, shields the crack tip driving force, thereby reducing the effective force for crack extension. Hence, the same effect is visualized as the compressive force in continuum mechanics. Thus, effects of the plastic zone persist during both loading and unloading either in terms of strain hardening or in terms of compressive residual stresses.

Several investigators [9–11] have attributed crack retardation to residual stresses ahead of the crack tip. Drew et al. [12] and Ling and Schijve [13] confirmed that residual stresses play a major role in the retardation by demonstrating that the effects can be eliminated by annealing after the overload. A phenomenological expression in terms of ΔK and $K_{\max}$ was developed by Wheeler [14] to quantify the overload effects. Schijve and others [15] have criticized Wheeler's model on the grounds that residual stresses affect both $K_{\max}$ and $K_{\min}$ equally, thus not affecting the crack driving force ΔK. Hence, they conclude that residual stresses do not affect directly the crack tip driving force. This statement is only partially true as will be discussed later. Fleck [4] raised several additional criticisms to the residual stress arguments: (a) Retardation should occur immediately after the overload because that is when the largest residual stresses are present whereas experimentally, delayed retardation is observed. (b) Observed retardation persists even after the crack has propagated out of the overload reverse plastic zone, beyond the region of overload-induced compressive residual stresses. (c) Mean stresses relax in the reversed plastic zone as the crack advances, hence, the full ΔK is experienced by the crack tip regardless of the sign and magnitude of the residual stresses.

The last two mechanisms (4) and (5) i.e. plasticity [16] and roughness induced closure, shift the attention to factors behind the crack tip. While we have consistently argued [17,18] that plasticity always opens the crack rather than closing the crack, Riemelmoser and Pippan [19] have recently presented an analysis that shows that plasticity in the crack wake can contribute to small amounts of closure. Since overload plasticity must occur ahead of the crack tip, plasticity induced closure does not manifest until the crack moves forward and the overload plastic zone is its wake. Thus the delayed retardation is conceptually in tune with plasticity induced closure. In addition, unlike the residual stresses, closure affects amplitude (not just K_{max}), thus reducing the crack tip driving force, measured in terms of ΔK. Furthermore, the plasticity-induced closure is likely to persist even after the crack grows out of the reversed plastic zone, since the contributing factor is the overload monotonic plastic zone. Plasticity induced closure has received considerable support in the fatigue community because of the above perceived limitations of the residual stress hypothesis. There are many experimental results [20–23] in the literature that attribute the retardation effects to plasticity induced crack closure.

Several authors [3,22,23] have attributed retardation effect to roughness induced closure. Roughness induced crack closure produces similar effects such as delayed retardation effects and the retardation effects beyond the reverse plastic zone. Roughness arises not from overload plasticity, per se, but from slip planarity and crack path tortuosity, and hence is expected to play a role in planar slip materials. Since overload effects are common across the board, it is unlikely that roughness induced closure is the general cause for the overload retardation effects. Materials that show a significant faceted mode of crack growth near the threshold region or a tortuous crack path can show larger retardation due to this roughness-induced closure. This closure contribution should be considered as additional superimposed effect over the other process of retardation. Besides, there is also a question of whether the roughness arising from crystallographic mode of cracking itself is an effect rather than the cause for retardation. In spite of that, roughness can still introduce secondary effects, further reducing the driving force. Our analysis [17] indicates that while the plasticity induced closure is unlikely, the roughness-induced closure is possible but that contribution is also very small.

Significant confusion and disagreements still exist in terms of the exact mechanism of retardation by overloads. Most investigators believe that plasticity induced closure is the major cause for retardation. However, many other investigators believe that compressive residual stresses are the primary cause for retardation. The issue is further complicated by the fact some attribute closure to combined plasticity in the wake and compression in the front of the crack. Major objections to residual stress arguments rest on the assumptions that (a) ΔK is the only crack tip driving force under fatigue (b) it is unaffected by residual stresses, (c) the residual stresses exist only within the reverse plastic zone and (d) delayed retardation is unaccountable by residual stresses. We will see later that there are problems in all these assumptions and some are not fully justified, particularly in view of the overwhelming experimental evidence that the residual stress effects are eliminated by annealing [12,13].

3. Unified approach to fatigue crack growth and role of internal stresses

At this stage, it is instructive to present our Unified Approach [24–28] for quantifying fatigue crack growth. We have shown analytically that the closure contribution is very small, much smaller than what has been believed. There is increasing experimental evidence that current ASTM recommended practices overestimate closure, and that the true effects are 20% of what has been estimated in agreement with our basic analysis. Hence, effects hitherto attributed to crack closure should be related to more intrinsic factors. In the Unified Approach, we have:

1. Fatigue is fundamentally a two-parametric problem because there are two driving forces required to obtain fatigue crack growth, K_{max} and ΔK.
2. There are two fatigue thresholds, $K^{*}_{max,th}$ and ΔK^{*}_{th} corresponding to two driving forces. These are asymptotic values in the ΔK–K_{max} plot. Both must be satisfied simultaneously for fatigue crack growth to occur.
3. Existence of dependence of ΔK_{th} on R is a trivial consequence of the existance of two thresholds. Extrinsic mechanisms (crack closure) therefore are not necessary to account for R dependence of ΔK_{th}.
4. If closure exists, then a third parameter, in addition to K_{max} and ΔK_{th}, would be needed to fully describe the fatigue process.
5. Crack growth is driven by total crack tip stresses, i.e., the superimposition of the externally applied stress and any internal stress that exist.
6. Internal stresses exist due to, for example, defects, scratches, inclusions, or other stress concentrators; residual stresses such as from welding or heat treatments, cold work, transformation induced stresses, and plasticity, including overload plasticity.

7. The basic effect of internal stress is to offset the total stress intensity at the crack tip relative to the externally applied stress, so that both K_{min} and K_{max} would generally be affected similarly. Consequently, the primary effects of internal stress manifest through K_{max} and not the ΔK parameter.
8. Environmental effects manifest primarily in the K_{max} term. This is because the K_{max} driving force is what opens and increments the crack, therefore it is more sensitive to environmental modification of the material at the crack tip.

We have called this the Unified Approach, since all the apparently disjointed phenomena, including anomalous effects of short crack growth and even the nucleation of cracks along the lines of the Kitagawa diagram [29], can all be combined under these unifying principles. Obviously, in view of the current discussion, the residual stresses generated due to overload plastic zones are internal stresses that affect the crack tip driving force. Since in the Unified Approach, K_{max} also enters as the major driving force for fatigue crack growth (in addition to the conventional parameter, ΔK), the arguments against residual stresses that they do not affect amplitude, ΔK, become irrelevant. In addition, K_{max} drives the monotonic plastic zone and hence residual stresses do not extend only in the reverse plastic zone. Reverse plastic zone is only one manifestation of the residual stresses and arises when the stresses locally exceed the material compressive yield stress; thus, it is a result rather than the cause of the residual stresses. Hence, this second objection to residual stresses is also untenable. The third objection that residual stresses do not account for delayed effect can also be ruled out once we understand the nature and profile of the residual stresses. Thus, the emphasis in the Unified Approach is to shift the major attention to factors ahead of the crack tip rather than to those behind the crack tip.

Recently, Lang and Marci [30–34] have done an elegant analysis of the role of plasticity to show what is ahead of the crack tip is more important than crack closure behind the crack tip, in agreement with our analysis. They have proposed new concepts involving K_{pr}, a stress intensity that must be overcome for the crack to move forward. We show here that their K_{pr} concept is consistent with our Unified Approach as a part of the K_{max} requirement. Their elegant and complimentary work on the role of K_{pr} and how it is affected by overloads blends naturally into our approach. Lately, Donald et al. [35–37] have proposed that K_{max} has to be included along with ΔK in the representation of crack growth data in some systems. We show that their analysis also is a subset of our general universal plot of ΔK–K_{max} in the description of the fatigue crack growth phenomena.

4. Crack closure, its measurement and its role

Since crack closure is attributed as one of the major causes for the retardation effects, it is instructive to examine the magnitude of crack closure and its relative role in the crack growth process. Existence of plasticity-induced crack closure has been severely questioned while asperity-induced closure, which includes roughness due to crack tortuosity, oxide or chemical reaction debris etc., has been shown to be small. Following our work, there has been intensive study to critically examine crack closure measurements. Detailed and careful analysis of crack closure measurements by Donald et al. [37] have shown that the current ASTM criteria for the determination of K-closure are flawed. They have proposed and discussed several alternatives. Paris et al. [38] have provided theoretical justification for the modified criteria for crack closure. Lang and Marci [31] have provided a simple estimation of crack closure, which is somewhat conservative. While the correct method for measuring crack closure levels has still not been identified, it is widely acknowledged that all methods used to date have tended to overestimate the crack closure levels. Here we propose a corrected crack closure measurement (CCCM) based on the shape of the load-displacement curve.

Fig. 2 show a magnified view of a typical load-displacement curve where the displacement is measured along the loading line. Based on the curve there are two parameters that can be defined, K_{op} and K_w. K_{op} corresponds to the first deviation from the linearity of the load-displacement curve during unloading, measured

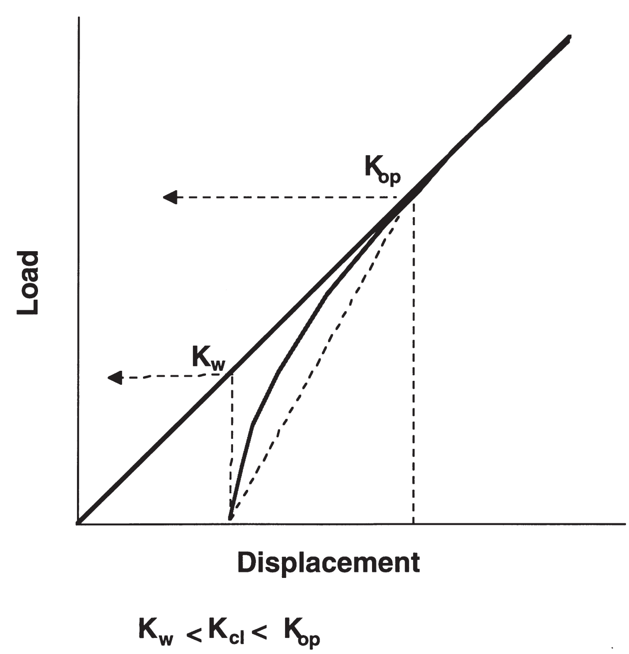

Fig. 2. Load–Displacement curve and corrected crack closure measurement (CCCM) using the load–displacement curve.

within some operationally defined percent deviation. This value, however, clearly over estimates closure in virtually all instances. If complete closure occurred at K_{op}, i.e., complete crack face contact, the load-displacement curve would drop sharply to it's crack-free value (zero in the absence of a notch). In the majority of cases, however, it decreases gradually and non-linearly indicating that the stress intensity acting on the crack tip also would be decreasing gradually to some value less than K_{op}. K_{op} therefore is an upper bound on the closure. At complete unloading, there is a net displacement of the crack surfaces indicative of remnant plastic strain. One can estimate the lower bound for crack closure, K_w, corresponding to the remnant plastic displacement. Lang and Marci [31] have used this to estimate crack closure and showed that crack closure is small and is negligible. The true value for closure should be in between the two limiting values K_{op} and K_w. Some investigations and approaches [30,37,38] seem to suggest that the true closure value is nearer to K_w than K_{op}, and in most experimental cases, K_w is less than 20% of K_{op}. Hence, we propose a simple inverse mean of the two limiting values as rough estimate of the true value of crack closure. Thus the corrected closure value, K_{ccl} is given by

$$\frac{1}{K_{ccl}}=\frac{2}{\left(\frac{1}{K_{op}}+\frac{1}{K_w}\right)} \qquad (1)$$

$$K_{ccl}=\frac{2K_{op}K_w}{K_{op}+K_w} \qquad (2)$$

The equation is naturally biased towards K_w. Thus, for a case where K_{op} is 10 MPa√m and K_w is 2 MPa√m, the corrected closure value is in between these two extreme values and the above equation gives K_{ccl}=3.3 MPa√m. For an ideal case, when K_{op} and K_w are equal, the equation correctly predicts that $K_{ccl}=K_{op}=K_w$. It is important to note that while the above equation provides a correction for the non-linear compliance relation observed experimentally after the first contact of the mating surfaces, this is a simple recipe but without any theoretical basis. True theoretical estimation is complicated by the non-linear distributed forces along the length of the crack. Paris et al. [38] and Donald et al. [35–37] have provided analytical and experimental variants of the crack closure estimations. While the true estimation of crack closure remains ambiguous, indications are that its value is much smaller than what has been assumed, and the load ratio dependence still remains after ΔK correction for crack closure under constant amplitude fatigue. Hence, closure cannot account for the overload effect.

5. Analysis of crack growth data and role of K_{max}

Since it has been recognized that the true crack closure contribution is either negligible or small at best, attempts have been made to explain the load-ratio dependence of ΔK_{th} by other ways. We had proposed that K_{max} is an important parameter and one has to consider both ΔK and K_{max} for complete description of fatigue crack growth. Recently Donald et al. [36] have analyzed their extensive crack growth data and plotted crack growth rate, da/dN in terms of

$$\frac{da}{dN}=C(\Delta K)^n(K_{max})^m, \qquad (3)$$

where constants m and n are related. The values of ΔK were used after correcting for crack closure. Their analysis points out that even after the correction of crack closure, there is a K_{max} dependence. In the above equation, $K_{max}>>\Delta K$ (particularly at high R values) while $m<n$. Here we want to point out two aspects of K_{max}: the crack growth rate dependence on K_{max} that is recognized in the above equation, and the limiting values of K_{max} for any crack growth including threshold that is not evident in the above equation. Essentially K_{max} and ΔK can not be less than some critical values, K^*_{max} and ΔK^*, respectively for a given crack growth rate and at threshold the limiting values converge to their respective thresholds, $K^*_{max,th}$ and ΔK^*_{th}. This is illustrated with reference to another set of data generated by Lang [30]. Lang reported extensive data for various constant R-ratios, and constant K_{max} tests for Al-7475-T7351 alloy in LT orientation.

Fig. 3 shows the ΔK–K_{max} plot at two different crack growth rates, one close to the threshold (da/dN=1×10^{-7} mm/cycle is considered by Lang as close to the material threshold) and the other at da/dN=5×10^{-5} mm/cycle. Note that all the data, whether at constant R or at constant K_{max}, fall on the same curves. Hence we call the ΔK_{th} vs. K_{max} the fundamental threshold curve describing the interplay of the two thresholds on crack growth. Clearly there are two thresholds — $K^*_{max,th}$ (2.25

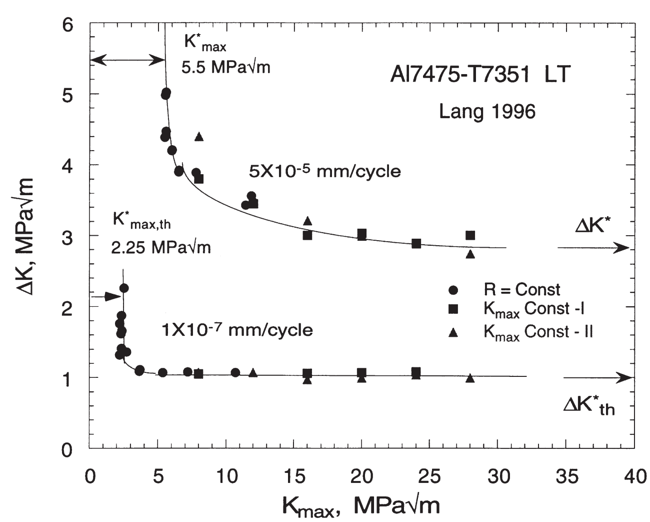

Fig. 3. ΔK–K_{max} plots Al-7475-T7351 alloy LT Orientation.

MPa√m for this alloy) below which no fatigue crack growth occurs for whatever the value of ΔK; and ΔK^*_{th} (1 MPa√m) below which no crack growth occurs whatever be the value of K_{max}. Importantly, such limiting values, K^*_{max} and ΔK^*, exist not only for threshold but also for any given crack growth rate. This is shown in Fig. 3 for $da/dN=5\times10^{-5}$ mm/cycle. These limiting relationships are not depicted in the continuos functional relationship represented in Eq. (3). The ΔK^*_{th} differs from the current understanding of ΔK_{th} since from Fig. 3 the later is not a single valued function and depends on K_{max}. Donald et al. [36] have noted that the ΔK–K_{max} curves are not a perfect L-shape but there is a continuous decrease of ΔK with increase in K_{max} value. In Fig. 3, at the threshold, the curve follows the perfect L-shape, but at higher growth rates there is a concave curvature in the ΔK–K_{max} curve. The nature of the curvature and the type of ΔK–K_{max} behavior have been discussed extensively in terms of various classifications [25]. The perfect L-shaped curve is defined as Type III behavior while the concave curvature is defined as Type II behavior. The Type II behavior has been attributed to plasticity effects either in terms of crack tip blunting or interactive effects of monotonic plastic zone with crack tip driving force. In Fig. 3, for this material, and for other ductile materials as well, with increasing crack growth rates, the behavior shifts from Type III to Type II. The same data in a log–log plot shows a linear relation, Fig. 4, indicative of the power law-dependence with K_{max} as exemplified by Eq. (3) by Donald et al. [36]. While the slope of the linear portion of the curve indicates ΔK–K_{max} power law relation, one should be aware that it is not the only K_{max} dependence that one is concerned in quantifying fatigue crack growth. The second is the asymptotic value of K_{max} for each crack growth rate. Thus with increasing crack growth rate from 1×10^{-7} to 5×10^{-5} mm/cycle, the K^*_{max} increases from 2.25 MPa√m to 5.5 MPa√m while the limiting value of ΔK increases from 1 MPa√m to 2.5–3.0 MPa√m. Thus to enforce a given crack growth rate, both asymptotic values need to be exceeded. Thus, K_{max} plays a role throughout the crack growth and not just only at high R-ratios.

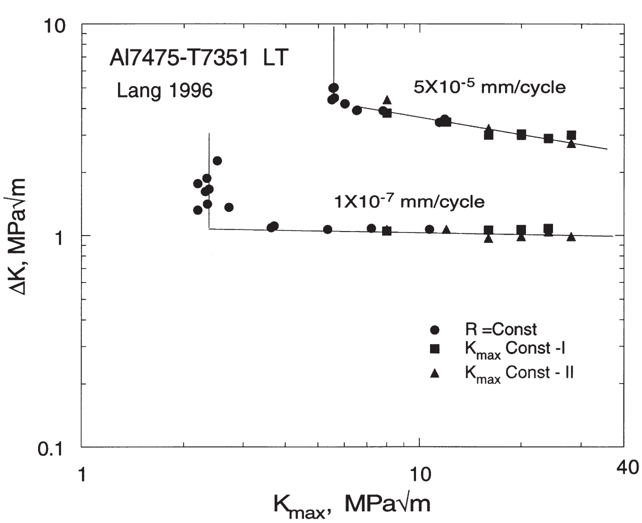

Fig. 4. Log–log plot of the data in Fig. 3 to show the exponential dependence on K_{max} at high R values.

The interactive term between ΔK and K_{max} increases with crack growth rate. This is shown in Fig. 5(a) and (b). Fig. 5(a) shows the log–log plot of ΔK vs K_{max} for various crack growth rates showing the nature of the relation, and in Fig. 5(b) the slope, the exponent from Fig. 5(a), is plotted as a function of da/dN. The effect saturates at high crack growth rate. The results indicate that Eq. (3) itself is an approximation for the non-linear interaction between the two load parameters. The implication is that the fitting of the data in some traditional power-law relations has its limitations because of the non-linear behavior due to interaction terms that can not be expressed in simple forms using linear fracture mechanics parameters. These limitations should not be attributed wrongly to the phenomenon of crack closure behind the crack tip. These second order effects are intrinsic in linearization of the problem that is intrinsically non-linear since fatigue is a plasticity induced damage process. For engineering applications one can use the power-law relations as long as one is aware of the limitations.

6. Crack propagation behavior in terms of K_{pr}

Before discussing overload effects in terms of the Unified Approach, it is instructive to investigate the new parameter K_{pr} that Lang and Marci have deduced using detailed and careful experiments. Lang and Marci outline that K_{pr} is not a crack closure parameter but is related to K_{max} required for crack propagation. It is instructive to inquire whether K_{pr} is a new parameter independent of ΔK and K_{max} that we have discussed above, and if not, how does K_{pr} fit in the ΔK–K_{max} curves discussed above, Fig. 3.

Fig. 6, taken from Lang [30], describes schematically the K_{pr} concept as well as the measurement technique for constant amplitude using the Crack Propagation Load Measurement (CPLM) method. After establishing steady state crack growth at given amplitude, ΔK, the specimen is next unloaded to K_{min}. A small K_{max} close to K_{min} was then selected and specimen was then subjected to a small ΔK (in our procedure it is ΔK^*_{th} which Lang and Marci call ΔK_T). The cycling is done for a maximum of 10^7 cycles to see if there is any detectable crack growth. If not, then K_{max} is raised by small increments, holding ΔK essentially constant, and the procedure is repeated until first noticeable crack growth occurs. It was found that one has to raise K_{max} to the level of K_{pr} before crack

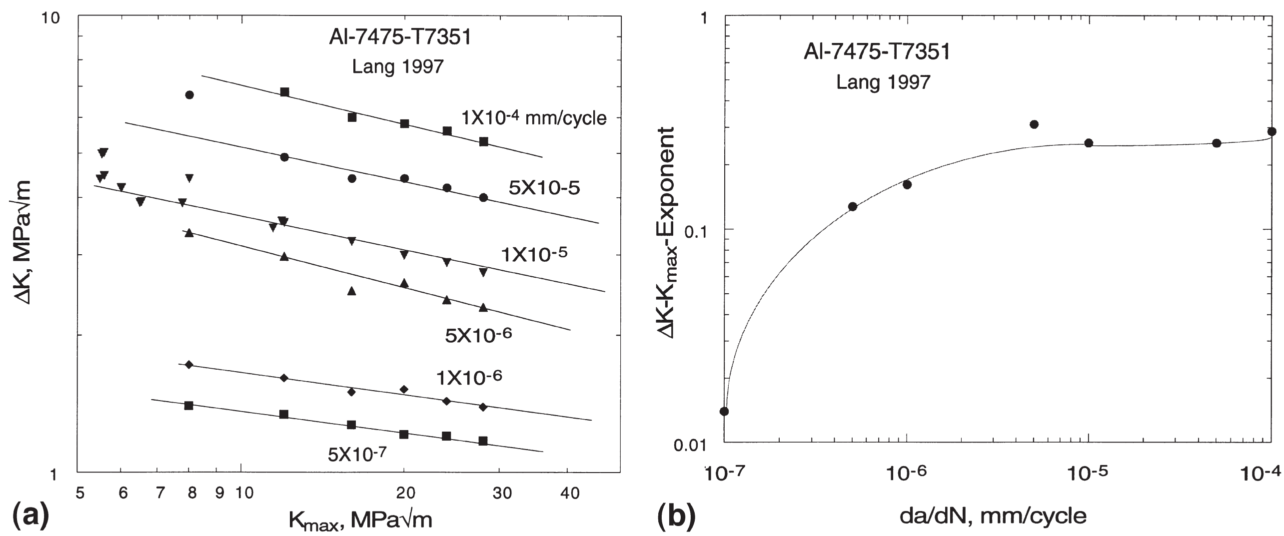

Fig. 5. (a) The exponential dependence is a function of crack growth rate. (b) The variation of the exponent with crack growth rate.

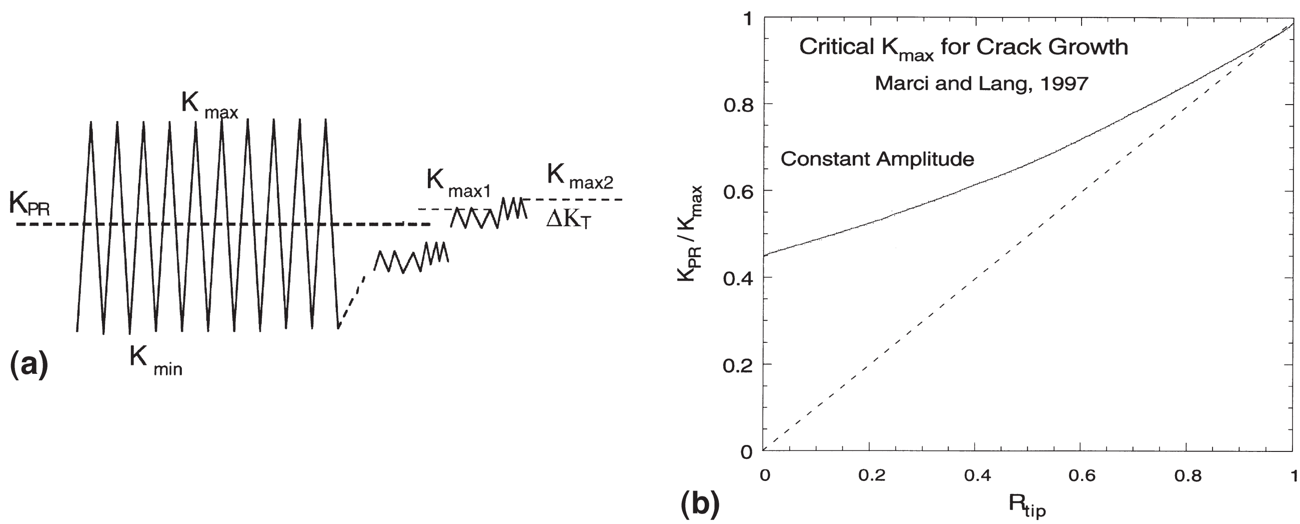

Fig. 6. Schematic illustration of the experimental determination of K_{pr} using Crack Propagation Load Measurement (CPLM) by Lang and Marci. (b) Variation of K_{pr} with R_{tip} where R_{tip} is the R-value corrected for crack closure.

begins to propagate. The value of K_{pr} depends on the background K_{max} and ΔK or load ratio for which the steady state conditions were originally established. The procedure they followed [30–34] is illustrated schematically in Fig. 6. Physically, for a given K_{max} and ΔK, there are two critical values in terms of peak stress intensity and amplitude below which crack growth does not occur. Lang and Marci [31] denote these as K_{pr} and ΔK_T. At the threshold, one expects their K_{pr} and ΔK_T to be related to the two thresholds K^{*}_{max-th} and ΔK^{*}_{th} under our Unified Approach. For Al 7475-T7351, they have determined K_{pr} as a function of the steady state K_{max} and R-ratio, and expressed their results in an empirical form,

$$K_{pr}=(0.455+0.321R_{tip}+0.208R_{tip}^{2})K_{max}, \quad (4)$$

where R_{tip} is the effective stress ratio at the crack tip, (which is not necessarily the same as the remote applied load ratio R).

The results for the alloy are represented in Fig. 6(b). It is interesting to note that the above equation is very similar to the empirical equation of crack closure proposed in the literature [16]. Lang and Marci [31] emphasized very clearly that K_{pr} is not related to crack closure behind the crack tip, but a required K to propagate the crack forward. It is the stress required to overcome the compressive stresses in front of the crack tip due to the background monotonic plastic zone. We now examine their K_{pr} in detail to see how it is related to K^{*}_{max}.

Fig. 7 shows the ΔK and K_{max} values at two crack growth rates, 1×10^{-7} and 1×10^{-5} mm/cycle, extracted from the raw da/dN data [30]. Note that Lang and Marci

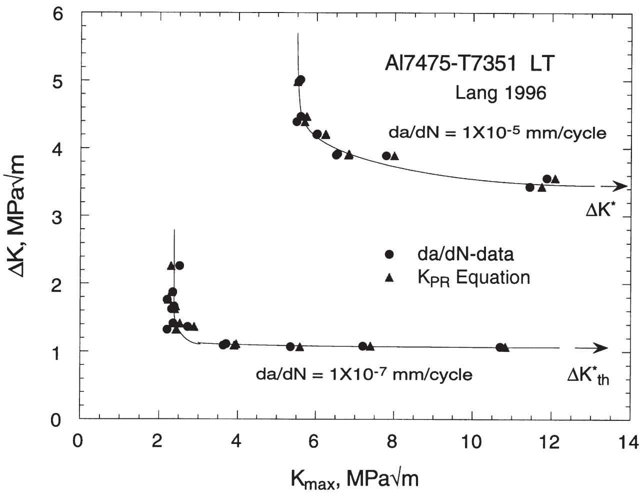

Fig. 7. Identity of ΔK–K_{max} extracted from the raw da/dN data and that from the empirical equation of K_{pr} determined independently by CPLM method. Experimental K_{pr} confirms independently the critical K_{max} required for crack growth and its relation to crack tip plasticity ahead of the crack tip.

[31] have determined K_{pr} values, Eq. (4), independent of the crack growth data. Using their equation, we can now calculate K_{pr} values for the two crack growth rates, assuming that R_{tip} is the same as R-remote (essentially closure is assumed to be negligible). From K_{pr} and ΔK_T values one can generate the ΔK–K_{max} curve from Eq. (4) and these calculated values are also plotted in Fig. 7. The two sets of data fall on the same curves, indicating that ΔK–K_{max} relation extracted from the raw da/dN data is identical to the ΔK–K_{max} relation extracted from Eq. (4) that outlines K_{pr} in terms of K_{max} and R. We can conclude that steady state K_{pr} values determined by Lang and Marci are the reflection of critical values, K^*_{max}, required to enforce a given rate of crack growth. Likewise, one should be able to extract K_{pr} values and the empirical relation, Eq. (4), directly from the raw da/dN data or ΔK–K_{max} plots, without the extensive experimental work.

This exercise proves several points we wish to emphasize.

1. ΔK–K_{max} relation is fundamental for a material, environment and crack growth rate.
2. Lang and Marci's analysis provides convincing, independent experimental proof that there is a K_{max} threshold that must be met in addition to a ΔK threshold.
3. Not only at threshold but also at any finite or non-zero crack growth rate, there are two limiting values of ΔK–K_{max} that must be exceeded to maintain that crack growth rate.
4. There are second order interactions between ΔK and K_{max} that can manifest the slope or curvature of ΔK–K_{max} curve, as shown by Donald et al. (Fig. 5).
5. Lang and Marci's experimental evaluation of K_{pr} and its consistency with our two-parameter requirement provide a strong independent support for the Unified Approach.
6. In addition, their analysis also elucidates the physical meaning of the K_{max} threshold. K_{max} has to exceed K_{pr} to propagate and its existence is related to (1) the residual stresses arising from the plasticity ahead of the crack tip and (2) intrinsic material resistance to cracking under cyclic loads. K_{pr} is inclusive of both since K to propagate a crack incrementally was determined.
7. Finally Fig. 7 shows that da/dN data determined at various R-constant and/or K_{max} constant tests is sufficient to extract the material behavior. For constant amplitude data, da/dN data can give complete information, including K_{pr}.
8. Lang and Marci have determined Eq. (4) after making correction to the crack closure values. Since the ΔK–K_{max} relation extracted from Eq. (4) fits right on the raw da/dN data without crack closure correction, this implies as ascertained in the Unified Approach that crack closure contributions are negligible. Note in Fig. 7 the data extracted from da/dN and K_{pr} are relatively shifted along the curve and this shift could be the result of the crack closure correction.
9. The empirical descriptions such as Eq. (4) are in fact the description of the interrelation between ΔK–K_{max} at various crack growth rates. ΔK^* values have to be known along with Eq. (4) to determine ΔK–K_{max} curves. ΔK^* values are obtained from da/dN–ΔK data at a high R-ratio.

The above analysis emphasizes by independent means that processes ahead of the crack tip are more important than those in the wake. This will have a direct bearing in the analysis of overload and underload effects.

7. Effect of overloads

As pointed out earlier, current explanations for overload effects rests on (a) plasticity induced closure and (b) residual stress effect. The major objection to residual stress arguments is that the stresses do not affect ΔK, which is the primary driving force for fatigue crack growth. The extended analysis presented above establishes emphatically that K_{max} also must be taken into consideration as the driving forces for crack growth in addition to ΔK, and K_{max} is affected by residual stresses. We address here how overload effects manifest in terms of K_{max}. Lang and Marci [33] have established, using their CPLM method, the effect of overloads and underloads on K_{pr}. Since K_{pr} is intimately related to the critical K_{max} required for crack growth, overload effects on K_{pr} should correspond directly to the effect of residual stresses on the critical K_{max} required for crack growth.

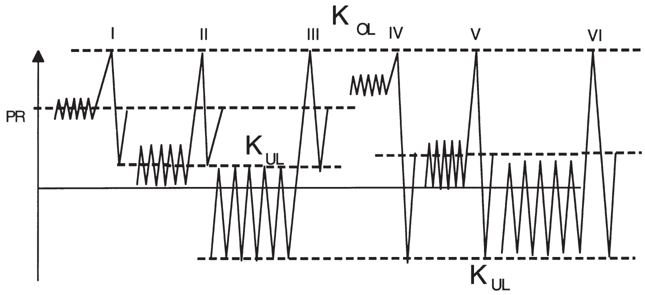

Fig. 8. Schematic illustration of K_{pr} for overload and under loads and its dependence on the K values at the spike loads, from Lang and Marci.

Fig. 8, from Lang and Marci [33], shows the relation between various types of single overload — underload combinations and the resulting value of K_{pr}. As indicated in the schematics, K_{pr} appears to depend solely on K_{max} and K_{min} loads during the overload — underload sequence. In the illustration, Cases I, II, II each having different background ΔK–K_{max}, will give rise to the same K_{pr}, since all of them have the same K_{max}–K_{min} during the overload–under load cycle. Similarly, Cases IV, V and VI have the same K_{pr}. Defining unloading ratio, U_R as $K_{min,ol}/K_{max,ol}$ — during the last overload–under load cycle, Lang and Marci have determined K_{pr} as function of U_R for the Al 7475-T7351, and presented the data as shown in Fig. 9. The constant amplitude K_{pr} from Fig. 7 is also shown for comparison. They have arrived at an empirical relation that best fits the data and the correlation function is similar to Eq. (4) and is given by,

$$K_{pr,ol}=(0.322+0.58U_R+0.241U_R^2-0.18U_R^3)K_{max,ol}. \quad (5)$$

Figs. 8 and 9 seem to emphasize that the $K_{pr,ol}$ depends only on the last overload–under load cycle and not on the prior background ΔK and K_{max}. However, the fact that the curve differs from the steady state K_{pr} is an indication that prior history has an effect, and the steady state plasticity conditions differ from the transient conditions from the spike loads. This can be understood in terms of steady state dislocation cell-structure that gets perturbed by the overload–underload cycle. To reestablish new steady state condition or to revert to prior steady state, many cycles are required. In fact, the subsequent repeated overload–underloads [33] reestablishes the new steady state condition that brings the K_{pr} back to that given by the steady state curve.

Further, it is important to note that the K_{pr} values in Fig. 9 for both the steady state and overload conditions correspond to the K_{max} required to propagate the crack immediately after the spike K_{max}–K_{min} loads, and not for the subsequent crack length increments. This has relevance for the overload cycle. As the crack moves further into the overload plastic zone, $K_{pr,ol}$ should change gradually towards the steady state condition. Obviously it will take N_d (delay cycles) for the crack to grow out of the transient regime reestablishing the steady state corresponding to the background K_{max}–ΔK. Hence, the technique of Lang and Marci is worth pursuing to determine $K_{pr,ol}$ as a function of crack length until $K_{pr,ol}$ approaches the steady state value. In principle, it should take N_d number of cycles for the $K_{pr,ol}$ curve to shift towards the K_{pr} steady state curve, and the trajectory of the $K_{pr,ol}$ as a function of number of cycles has to be quantified to use this approach for life prediction.

Recognizing thus that Eq. (5) provides the maximum $K_{pr,ol}$ value immediately after the spike load, one can determine the effect of overload on the ΔK–K_{max} behavior, along the similar lines in Fig. 7. The effect calculated based on Eq. (5) is shown in Fig. 10 for two overload ratios, 1.5 and 2.0, for Al7475-T7351 at a crack

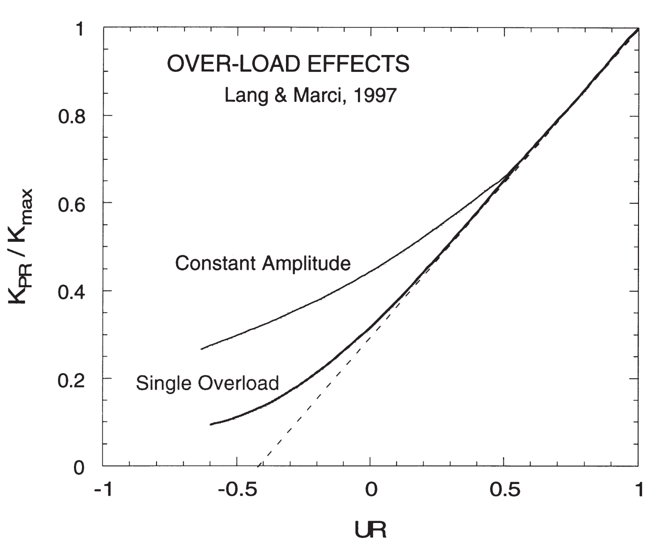

Fig. 9. Effect of overload on K_{pr} in comparison to its steady state K_{pr} value.

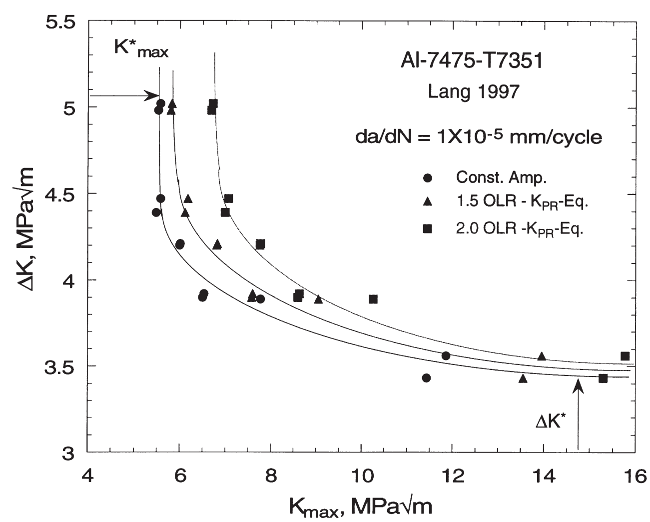

Fig. 10. Demonstration of how overload K_{pr} affects ΔK–K_{max} curves by shifting the curves to the right due to the compressive residual stresses affecting crack tip driving force, K_{max}. Equivalence of the two approaches is shown.

growth at 5×10^{-7} mm/cycle. With increasing overload ratio, the ΔK–K_{max} curve shifts to the right indicating that because of residual compressive stresses, the critical K_{max} required to cause crack growth rate of 5×10^{-7} mm/cycle increases. While the critical ΔK^{*} required for crack growth also increases with overload, this increase is very small, within the limits of experimental error.

Thus while the criticism that the residual compressive stresses do not significantly affect the amplitude, ΔK, is appropriate, it is clear that compressive stresses significantly affect the critical K_{max} required for the crack growth. In fact, all superimposed non-cyclic type of stresses affect fatigue crack growth through K_{max}. Hence, any fatigue life prediction methodology is invalid or incomplete, unless the role of K_{max} is fully recognized and quantified. It is to be noted that crack arrest phenomenon, decelerating cracks even with increasing ΔK, non-propagating cracks, etc., are all manifestation of the changing internal stresses and the presence of K_{max} threshold. The nature of the internal stress gradients and the role of K_{max} need to be understood and quantified for development of reliable life prediction methods. In Fig. 10 with increasing overload ratio, the curves shift to the right since additional internal stresses due to overload plasticity have to be overcome. The extent of the ΔK–K_{max} curve shift in Fig. 10 depends on the magnitude of the residual stresses that are generated ahead of the crack due to overload, background ΔK and K_{max}, and material flow properties (flow stress, work hardening behavior, slip character, ease of cross slip, etc.,).

We have studied experimentally the effect of single overloads on the ΔK–K^{*}_{max} curve for a Al-7075-T6 alloy for 100% and 200% overloads, and the results are shown in Fig. 11. The data correspond to the near threshold condition where applied loads have to be increased in order to initiate crack growth after the overload. The results in Figs. 10 and 11 are similar, confirming again that the K_{pr} approach is just a different way of establishing the ΔK–K_{max} required for crack growth. Lang and

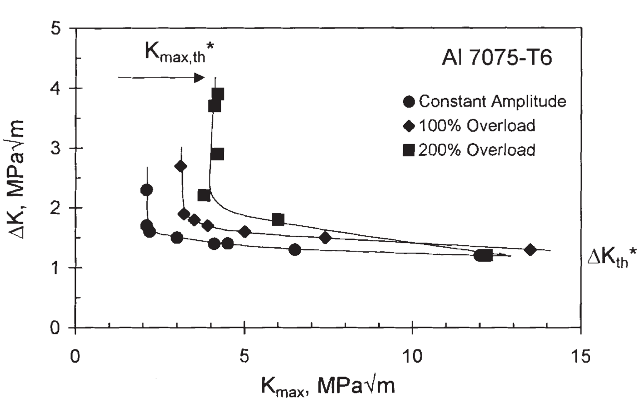

Fig. 11. Independent evaluation of overload effects on the ΔK–K_{max} curve for a Al-7075-T6 alloy at two overload ratios. The curves shift to the right as illustrated in Fig. 10.

Marci's work further confirms that crack closure contributions are negligible and the effect of the overload arises mainly from the residual stresses from the overload plastic zone, in agreement with the Unified Approach.

As stated earlier, Figs. 10 and 11 do not give complete transient behavior other than the peak effect of the spike loads. To establish the complete transient state, one has to investigate fully the changes in crack growth rate after the spike load. We discuss here the work of Bray [1] on the effect of overloads. Using his base line crack growth data and the changes in the crack growth rates, one can extract the residual stress profile after overload. Fig. 12(a) shows schematically the procedure for extracting the residual stresses. The procedure is similar to the internal stress concept used to understand the growth behavior of the short cracks. Fig. 12(b) shows the actual data for AA8022 Aluminum alloy at ambient conditions for several overload conditions and back ground R-values. Several key points should be noted: (a) The maximum effect of overload is experienced by the crack, not immediately at the overload position, but at a short distance ahead of the original crack position. This has been referred to as delayed retardation and has been used as an argument to dismiss the residual stresses as the major factor for retardation. (b) This delayed distance depends very weakly on the overload ratio and the background R-value. (c) The residual stresses after reaching a peak decrease initially logarithmically with distance away from the point of spike load position, and then more rapidly with further increase in crack length. This can be seen more clearly in Fig. 12(c) where the absolute value of residual stresses are plotted with distance in a log–log scale. The changes in residual stresses are functions of the overload ratio and the background values of ΔK and R. The rapid drop in the stresses at larger distances could be the reflection of the dynamic changes in the overload plastic zone that interacts with the steady-state plastic zone that forms continuously with increase in crack length. (d) Due to dynamic interaction between the overload plastic zone and newly forming plastic zones with incremental crack length, the exact nature of the residual stress profile can be difficult to predict or quantify.

The question now that remains to be answered is whether the delayed peak effect is a sufficient ground to dismiss the residual stress argument. To answer this, we will consider here a simple case of the effect of dislocations ahead of the crack tip on the crack tip driving force. The plastic zone can, in principle, be replaced by a distribution of dislocations that resemble an inverted pile-up. The length of the pile-up is equal to the plastic zone size. As a further approximation, the pile-up itself can be replaced by a single superdislocation of strength equal to the sum of the Burgers Vectors of all the dislocations in the pile-up. The Burgers Vector of the super-

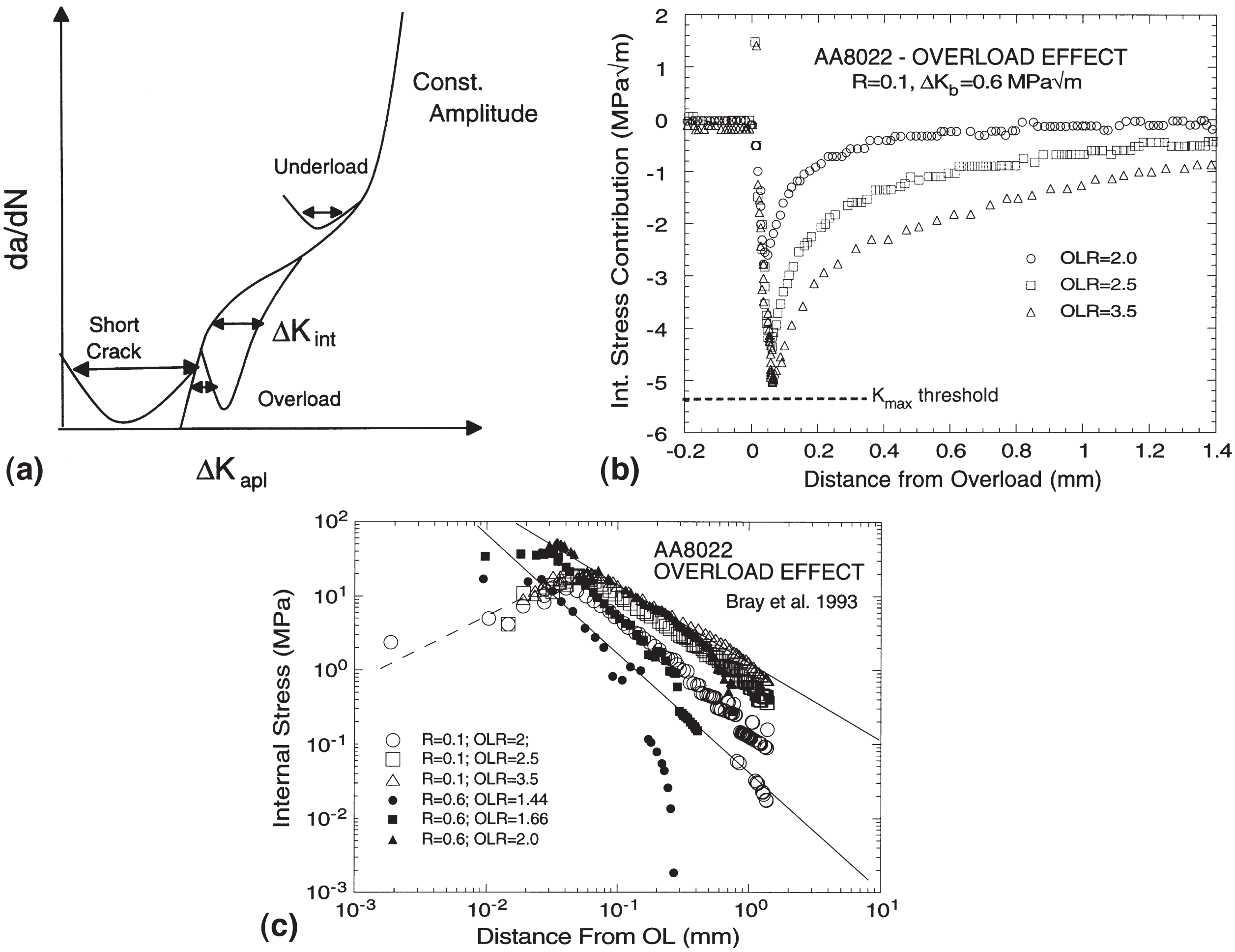

Fig. 12. (a) Schematic illustration for extracting internal or residual stresses from da/dN curves. (b) The residual stress profile as a function of incremental crack length for an AA8022 Aluminum alloy. (c) Residual or internal stresses as a function of crack increment on a log–log scale.

dislocation, N_b, is related to the crack tip opening displacement. While the problem is overly simplified, as we shall see, it captures its essence at least qualitatively. Fig. 13 shows the effect of a dislocation on the crack tip driving force expressed as K_d, the stress intensity factor due to a dislocation stress field. K_d term is normalized by a constant A, which contains Burgers vector and the elastic modulus terms. This K_d factor exerts the retarding force on the crack tip, reducing the crack growth rates or even causing crack arrest if the total K becomes less than the $K^*_{max,th}$. Fig. 13 was obtained using Lin–Thomson equation (Equation 46 of Reference [39]) for a dislocation with Burgers Vector 45° to the crack plane. The crack tip provides the reference coordinates. As the dislocation approaches from far right (or equivalently as the crack moves forward at a constant applied K), the retarding force (shielding force) on the crack tip due to the dislocation increases and reaches a maximum and then decreases. For this particular Burgers Vector, the sign of the force changes as the dislocation goes behind the crack tip. The dislocation crack interaction is such that the maximum shielding effect occurs not at the ori-

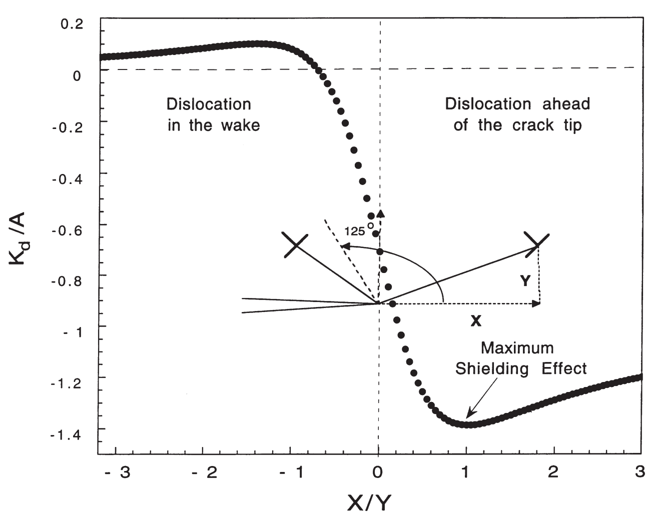

Fig. 13. Shielding effect of a dislocation ahead of the crack tip showing that maximum compression force occurs not at the crack tip but at a distance from the crack tip.

gin but a distance away from the crack tip, when the dislocation is still ahead of the crack tip. Since the dislocations spread out to the limit of the plastic zone, the integrated effect of all the dislocations, on the basis of Fig. 13, is expected to be not at the crack tip but a distance ahead of the crack tip. The distance where this maximum occurs depends on the pile-up length and the center of gravity of the pile-up in relation to crack tip coordinates.

It is important to note also that the maximum shielding occurs while the dislocations are still ahead of the crack tip, not when they are behind the crack tip. This implies that the maximum retardation should occur while the overload plastic zone is still in front of the crack tip in contrast to the plasticity-induced crack closure that should reach a maximum only when the center of the gravity of the pile-up moves behind the crack tip. Fig. 13 also indicates that the dislocation retarding force reduces rapidly as the dislocation moves behind the crack tip and for this particular orientation of Burgers Vector it even contributes to a force which is tensile rather than compressive. This proves further that retardation effect cannot be attributed to plasticity- induced closure.

Based on the dislocation analogy, the delayed effect is therefore justified due to the nature of the stress field of the dislocations and the dislocation distribution in the plastic zone; therefore the delayed effect by itself is not an argument against the residual stresses. The analysis confirms that the plasticity ahead of the crack tip is the major cause for the overload retardation and arises from the change in the stress state ahead of the crack tip and not due to the closure behind the crack tip.

Immediately after the application of high overloads, an initial acceleration of crack growth is encountered in some materials that are significantly damaged by the overload plastic strains right at the crack tip, Fig. 1(c). Large strains approaching the fracture strains at the crack tip can cause excessive damage aiding the accelerated crack growth. If the crack growth occurs by blunting process, then initial increase in crack tip blunting due to overload plastic strain also accounts for the increase in crack growth rates. Once the crack grows beyond this intensive plastically strained region, the elastic stresses due to dislocations in the plastic zone play a role in retarding the crack tip driving forces.

8. Summary and conclusions

We have examined the overload effects on fatigue crack growth and the contributing factors for these overload effects. Residual stresses due to the overload plastic zone are shown to be a major factor that contributes to retardation, rather than the crack closure behind the crack tip due to plasticity. The arguments that have been advanced in the literature against residual stresses, that they do not affect the cyclic amplitudes, is shown to be impertinent since the residual stresses affect K_{max}, which is also a driving force for fatigue crack growth. Our Unified Approach involving ΔK–K_{max} is discussed in the light of the new analyses by Lang and Marci [33] and Donald et al. [36] and it was shown that these analyses are consistent with the Unified Approach. Further, Lang and Marci's work on K_{pr} provides an independent validation for our Unified Approach to fatigue crack growth involving two driving forces and two thresholds. It is shown that their K_{pr} is related to our K_{max} threshold. That it is affected by overload residual stresses naturally follows. Thus, the current analysis of the overload effects and our previous short crack growth analysis [28] together confirm: (a) the validity of the two parametric requirement, ΔK and K_{max}, (b) insignificance of the role of closure contributions for a general case, and (c) the role of residual or internal stresses in understanding the fatigue crack growth behavior in a component. It is important to extend the analysis further to quantify the load–load interactions as they affect the local K_{max} values in order to develop more reliable fatigue life prediction methods for a component subjected to spectrum loads.

References

[1] Bray GH. Fatigue crack retardation in PM aluminum alloys AA8022 and AA5091. PhD. Dissertation, University of Virginia, 1993.

[2] Taylor D, Staniaszek IAN, Knott JF. When is a crack not a crack — Some data on the fatigue behavior of cracks and sharp notches. Int J of Fatigue 1990;12:397–402.

[3] Suresh S. Micromechanisms of fatigue crack growth retardation following overloads. Eng Fract Mech 1983;18:577–93.

[4] Fleck NA. Influence of stress state on crack growth retardation. In: Fong JT, Fields RJ, editors. Basic Questions in Fatigue, ASTM STP 924, vol. 1. ASTM, 1988:157–83.

[5] Sadananda K. Advances in fracture research. New York: Elsevier, 1986.

[6] Bucci RJ, Thakker AB, Sanders TH, Sawtell RR, Staley JT. In: Bryan DF, Potter JM, editors. Effect of load spectrum variables on fatigue crack initiation and propagation, ASTM STP 714. ASTM, 1980:41–78.

[7] Vasudevan AK, Sadananda K, Rajan K. Role of microstructures on the growth of long fatigue cracks. Int Jnl of Fatigue 1997;19:S151–60.

[8] Knott JF, Pickard AC. Effect of overloads on fatigue crack propagation - Aluminum alloys. Met Sci 1977;11:399–404.

[9] Schijve J. Fatigue crack propagation in alloy sheet material and structure. In: Advances in Aeronautical Sciences, vol 3, Pergamon, 1962:387–408.

[10] Donald DR, Anderson WE. Crack Propagation behavior of some airframe materials. In: Proceedings of the Crack Propagation Symposium — Cranfield, England, vol 2. 1961/1962:375–441.

[11] Brown RD, Weertman J. Effects of tensile overloads on crack closure and crack propagation rates in 7050 aluminum. Eng Fract Mech 1978;10:867–78.

[12] Drew M, Thompson KRL, Keys LH. The effect of overloads on fatigue crack propagation in offshore structural steels. In: Gifkins

RC, editor. Strength of Metals and Alloys (ICSMAG), vol. 2. Pergamon Press, 1982:867–73.
[13] Ling MR, Schijve J. The effect of intermediate heat treatments on overload induced retardations during fatigue crack growth in an Al alloy. Fat Fract Eng Mat Struct 1992;15:421–30.
[14] Wheeler OE. Spectrum loading and crack growth. Transactions of the ASME Series D, Jnl of Basic Eng 1972;94:181–6.
[15] Schijve J. In: Ritchie RO, Starke EA JR, editors. Fatigue 87, vol. 1. UK: Engineering Advisory Materials Service Ltd, 1987:1685–721.
[16] Elber W. The significance of fatigue crack closure. In Damage Tolerance in Aircraft Structures, ASTM STP 486. ASTM, 1971:230–242.
[17] Louat N, Sadananda K, Duesbery M, Vasudevan AK. A theoretical evaluation of crack closure. Met Trans 1993;24A:2225–32.
[18] Sadananda K, Vasudevan AK. Discussion of error in the analysis of the wake dislocation problem. Met Trans A 1998;29A:1359–60.
[19] Riemelmoser FO, Pippan R. Met. Trans. A. 1999 (in press).
[20] Trebules VW Jr, Roberts R, Hetzberg RW. In: Progress in Flaw Growth and Fracture Toughness Testing, ASTM-STP 536. ASTM, 1973:115–146.
[21] Reynolds AP. Constant amplitude and post-overload fatigue crack growth behavior in PM aluminum alloy AA-8009. Fat Fract Eng Mat Struct 1992;15:551–62.
[22] Phillips EP. NASA Technical Memorandum 101601, Langley Research Center, Hampton, VA, 1989.
[23] Ward-Close CM, Ritchie RO. In: Newman JC Jr, Elber W, editors. Mechanics in Fatigue Crack Closure, ASTM STP 982. ASTM, 1988:529–35.
[24] Sadananda K, Vasudevan AK. Analysis of fatigue crack closure and thresholds. In: Erdogan R, editor. Fracture Mechanics, vol. 25, ASTM STP 1220. ASTM, 1993:484–501.
[25] Vasudevan AK, Sadananda K. Classification of fatigue crack growth behavior. Met Trans A 1995;26A:1221–34.
[26] Sadananda K, Vasudevan AK. A unified framework for fatigue crack growth. In: Lutjering G. Nowack H, editors. Fatigue 96, vol. 1. Berlin: Pergamon, 1996:375–80.
[27] Sadananda K, Vasudevan AK. Short crack growth behavior. In: Piascik RS, editor. Fatigue and Fracture Mechanics, vol. 27, ASTM STP 1296. ASTM, 1997:301–16.
[28] Sadananda K, Vasudevan AK. Short crack growth and internal stresses. Int Jnl of Fatigue 1997;19:S99–109.
[29] Kitagawa H, Takahashi S. Trans Japan Soc Mech Eng 1979;45:1289.
[30] Lang M. Quantitative Untersuchung Von Reihenfolgeeinflussen auf Ermudungsrißfortschritt. PhD. Dissertation, Institue fur Werkstoff-Forschung, 1996.
[31] Lang M, Marci G. Reflecting on the Mechanical Driving Force for Fatigue Crack Propagation. In: Panontin TL, Sheppard SD, editors. Fatigue and Fracture Mechanics, vol. 29, ASTM STP 1332, ASTM, 1998 (in press).
[32] Marci G. A fatigue crack growth threshold. Engineering Fracture Mechanics 1992;42:367–85.
[33] Lang M, Marci G. The influence of single and multiple overloads. Eng. Fract. Mech. 1999: (in press).
[34] Lang M. Description of load interaction effects by the ΔK_{eff}-concept. 2nd Symposium on Advances in Fatigue Crack Closure Measurement and Analysis, ASTM-STP 1343. ASTM, 1998, (in press).
[35] Donald JK, Bray GH, Bush RW. An evaluation of the adjusted compliance ratio technique for determining the effects of stress intensity factor. In: Panontin TL, Sheppard SD, editors, Fatigue and Fracture Mechanics, vol 29, ASTM STP 1332. ASTM 1998: (in press).
[36] Donald JK, Bray GH, Bush RW. Introducing the K_{max} sensitivity concept for correlating fatigue crack propagation. In: Soboyejo WO, Srivatsan TS, editors., High Cycle Fatigue of Structural Materials: Symposium Proceeding in Honor of Professor Paul C. Paris. Warrendale, PA:TMS, 1998:123–141.
[37] Donald JK, Connelly GM. The Effects of Overloads on the Intrinsic Fatigue Crack Growth Rate Curve. In: Fatigue Damage of Structural Materials II, Cape Cod, Massachussetts, September 1998. (this symposium).
[38] Paris P. Service load fatigue damage — A historical perspective. In: Fatigue Damage of Structural Materials II, Cape Cod, Massachussetts, September 1998 (this symposium).
[39] Lin IH, Thomson R. Overview No. 47 — Cleavage, dislocation emission, and shielding for cracks under general loading. Acta Met et Mat 1986;34:187–206.